Linear propagation of light investigated with a white-light Michelson interferometer

Takao Fuji, Motohisa Miyata, Sakae Kawato, Toshiaki Hattori, and Hiroki Nakatsuka

Institute of Applied Physics, University of Tsukuba, Tsukuba, Ibaraki 305, Japan

Received June 7, 1996; revised manuscript received October 23, 1996

Linear propagation of light was investigated by using a white-light Michelson interferometer. This method gives the full information on the deformation of broadband optical pulses by the passage through samples in the linear regime. We observed the delay of pulse propagation for cobalt chloride in pyridine, free-induction decay signal for oxazine 1 in methanol, and the increase of peak velocity for nigrosine in water. By Fourier analysis of the interferograms, complex optical constants of the samples were also obtained. © 1997 Optical Society of America [S0740-3224(97)01805-5]

1. INTRODUCTION

The progress of ultrashort-pulse laser technology has enabled us to study ultrafast phenomena occurring in the femtosecond regime.[1] Great care must be taken in producing or handling ultrashort laser pulses because the dispersion of optical elements causes the deformation of pulse shapes. It is well known that in the linear regime we can predict the deformation if we have the full information on absorption and refractive-index spectra of the sample.

Recently, white-light Michelson interferometers were used to measure the group delay or the dispersion of laser cavities and optical components for femtosecond optical pulse generation.[2–5] Fourier transform spectrometers (FTS), which are common in infrared regions, use Michelson interferometers. But in almost all the commercially available FTS's the sample is inserted behind the output side of the Michelson interferometer, and the autocorrelation interferogram of the transmitted light is obtained. To measure the dispersion or the spectrum of refractive index, we have to insert the sample into only one arm of the Michelson interferometer and obtain not only the autocorrelation interferogram of the incident light but also the cross-correlation interferogram between the incident light and the transmitted light.

In the linear regime, we can see the pulse deformation by comparing the autocorrelation and cross-correlation interferograms. If the waveform of the incident light is the autocorrelation, then the waveform of the transmitted light is the cross correlation.[2–5]

In the present experiment we used the white-light Michelson interferometer in the study of the deformation of broadband optical pulses by the passage through samples with a different kind of dispersion.

2. EXPERIMENTAL SYSTEM

A schematic diagram of the experimental system is shown in Fig. 1. The input light source was a normal incandescent lamp with a power consumption of 650 W. The unpolarized light from the lamp was guided to a vibration-isolated bench through a multimode optical fiber with a core diameter of 0.9 mm. We used the very-large-core-diameter fiber to utilize as much light power as possible and to increase the signal-to-noise ratio even in the measurement of the interferograms of strongly light-absorbing samples. The light output from the fiber was collimated by a lens and was passed through a Michelson interferometer composed of a nonpolarizing beam-splitter cube and two corner-cube prisms. Since the light source is an incoherent incandescent lamp, the coherence area is much smaller than the beam cross section; therefore we need to make adjustments so that the same areas of the two beams from the both arms overlap spatially. The path length of one arm of the interferometer was modulated at $f = 1-2$ kHz by a piezoelectric actuator with the amplitude of ~250 nm. The path length, or the delay time τ, of the other arm was changed by a corner-cube prism moved on a translation stage with a stepping motor. The light output from the interferometer was detected by a photomultiplier tube and fed into a lock-in amplifier.

We measured two kinds of interferograms: one is the autocorrelation, $C_A(\tau)$, of the input light, and the other is the cross correlation, $C_C(\tau)$, between the input light and the light transmitted through the sample. As is shown in Fig. 1, two other interferograms were simultaneously monitored with the above-mentioned interferograms. The first is the autocorrelation interferogram of the light from a He–Ne laser, and it was used for calibration of the path length. The second is that of the white light that did not pass through the sample, and it was used to identify the position where the path-length difference between the two arms is zero.

3. THEORETICAL CONSIDERATION

The autocorrelation interferogram $C_A(\tau)$ is written as

$$C_A(\tau) = \langle E^*(t)E(t+\tau)\rangle, \tag{1}$$

0740-3224/97/0501074-05$10.00

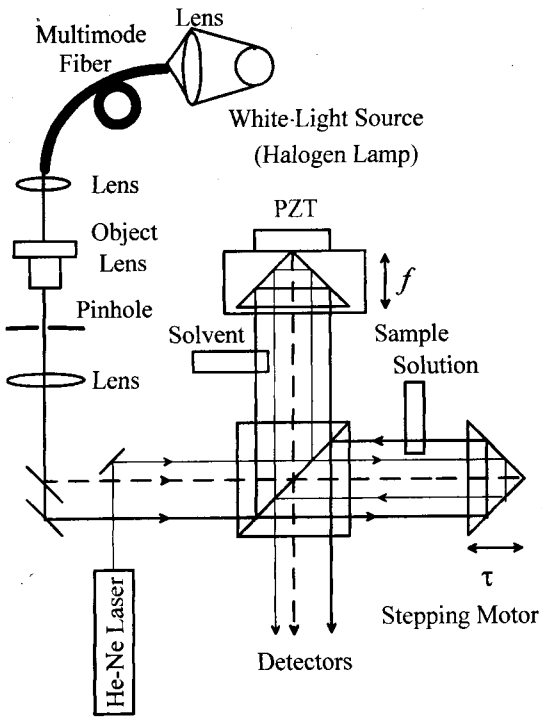

Fig. 1. Schematic of the white-light Michelson interferometer.

where $E(t)$ is the electric field of the white light and $\langle\ \rangle$ denotes time average. In the linear response approximation the electric field of the light transmitted through the sample, $E'(t)$ becomes as

$$E'(t) = \int_{-\infty}^{\infty} dt' h(t - t') E(t'), \tag{2}$$

where $h(t)$ is the response function of the sample. The cross-correlation interferogram, $C_C(\tau)$, between the input light, $E(t)$, and the output light, $E'(t)$, from the sample is written as

$$C_C(\tau) = \langle E^*(t) E'(t + \tau) \rangle. \tag{3}$$

If we insert Eq. (2) into Eq. (3), $C_C(\tau)$ becomes

$$C_C(\tau) = \int_{-\infty}^{\infty} d\tau' h(\tau - \tau') C_A(\tau'). \tag{4}$$

By comparing Eqs. (2) and (4), we can say that if the waveform of the light input to the sample is the autocorrelation $C_A(\tau)$, then the waveform of the output from the sample is the cross correlation $C_C(\tau)$. Therefore, in the linear regime, we can see the deformation of ultrashort light pulses by propagation through samples with a white-light Michelson interferometer.

On the other hand, Fourier analysis of the autocorrelation and cross-correlation interferograms gives us complex transmission coefficients of samples without relying on the Kramers–Kronig relation. By Fourier transformation of Eq. (2) we obtain

$$\tilde{h}(\omega) = \tilde{E}'(\omega)/\tilde{E}(\omega), \tag{5}$$

where $\tilde{E}(\omega)$ and $\tilde{E}'(\omega)$ are the Fourier transforms of the input field, $E(t)$, and the output field, $E'(t)$, respectively, and $\tilde{h}(\omega)$ is the Fourier transform of the impulse response function, $h(t)$, and is called the complex transmission coefficient. The Fourier transformation of Eq. (4) yields a relation similar to Eq. (5):

$$\tilde{h}(\omega) = \tilde{C}_C(\omega)/\tilde{C}_A(\omega), \tag{6}$$

where $\tilde{C}_A(\omega)$ and $\tilde{C}_C(\omega)$ are the Fourier transforms of the autocorrelation, $C_A(\tau)$, and the cross correlation, $C_C(\tau)$, respectively.

Because we measured the signal with a lock-in amplifier by using path-length modulation, our interferograms are not the autocorrelation or the cross correlation in a strict sense. Both the autocorrelation and the cross-correlation functions are modified from the true correlation functions in the same way as described by the following relation:

$$\tilde{C}'(\omega) = 2iJ_1\left(\frac{A\omega}{c}\right)\tilde{c}(\omega). \tag{7}$$

Here $\tilde{C}(\omega)$ and $\tilde{C}'(\omega)$ are the Fourier transform of the true correlation and that of our interferogram for either the autocorrelation or the cross correlation. $J_1(A\omega/c)$ is the first-order Bessel function, where A is the path-length modulation amplitude and c is the light velocity. Since $J_1(z)$ is proportional to z in the lowest order of z, we see that when the path-length modulation amplitude, A, is much smaller than the wavelength of light, λ; that is,

$$A \ll \lambda. \tag{8}$$

Our interferogram, $C'(\tau)$, corresponds to the time derivative of the true correlation function, $C(\tau)$. By using Eq. (7), we can get the relations for our interferograms:

$$\tilde{h}(\omega) = \tilde{C}'_C(\omega)/\tilde{C}'_A(\omega), \tag{9}$$

$$C'_C(\tau) = \int_{-\infty}^{\infty} d\tau' h(\tau - \tau') C'_A(\tau'), \tag{10}$$

which are exactly the same relations as Eqs. (6) and (4), respectively, for the true correlation functions. In this sense we can consider our interferogram autocorrelation or cross correlation. For simplicity, in the following discussion we call the measured interferograms the autocorrelation or the cross correlation.

4. EXPERIMENTAL RESULTS AND DISCUSSION

In the present experiment we studied the linear propagation of light through three kinds of solution by using the white-light Michelson interferometer. In the measurement of the autocorrelation the same type of glass cell (inner width 2 mm), containing only the solvent, were inserted into both arms of the interferometer. The solvents used were transparent in the visible region. We obtained the cross correlation by replacing the solvent in the glass cell in one arm of the interferometer with a sample solution. In this way, there was compensation for the change in the optical path length due to the glass cell and the solvent.

The first sample solution we measured was cobalt chloride, $CoCl_2$, in pyridine. The absorption of $CoCl_2$ in pyridine falls outside the spectral region of the measure-

ment. The autocorrelation and cross-correlation interferograms obtained with the white-light Michelson interferometer are shown in Fig. 2. We can consider the autocorrelation and the cross correlation to be the light waveforms of the input and the output, respectively. In this case we see that the delay of the pulse increases with the increase of the concentration of $CoCl_2$. This is reasonable if the refractive index becomes higher when the solute concentration increases. Figure 3 shows the change of the refractive index from pure pyridine to the pyridine solution of $CoCl_2$ given by Fourier transformation of the measured interferograms. This shows not only that the refractive index increases with the increase of the solute concentration but also that the refractive index monotonically increases with optical frequency. This feature clearly shows that there is a large absorption in the ultraviolet region that is outside of the spectral region of our measurement. However, we could not see any sign of this absorption in the absorption spectrum in the same spectral region.

The second sample solution was oxazine 1 in methanol. The absorption spectrum of oxazine 1 in methanol (1.2×10^{-4} M) is inside the spectral region of the measurement as shown in Fig. 4. It is well known that the power spectrum of light is given by the Fourier transform of the autocorrelation of the light field. But in the present experiment the spectral region of the measurement is determined not only by the power spectrum of the incandescent lamp but also by the characteristics of the optical elements and the detector in the experimental system, and it is given by the Fourier transform of the measured autocorrelation interferogram. The autocorrelation and the cross correlation are shown in Fig. 5. There is a slowly decaying tail in the cross correlation or the waveform of the output. This is called the optical free-induction decay signal.[6,7]

The resonant incident light excites the oxazine 1 molecule to induce the coherent oscillation of the electric dipole moment. The light emitted from this dipole moment is out of phase by π with respect to the incident light and

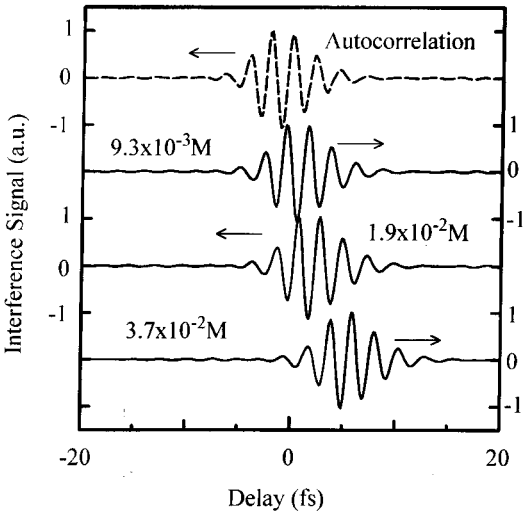

Fig. 2. Autocorrelation (dashed curve), and cross correlation (solid curves) of $CoCl_2$ in pyridine. The concentrations of $CoCl_2$ are indicated.

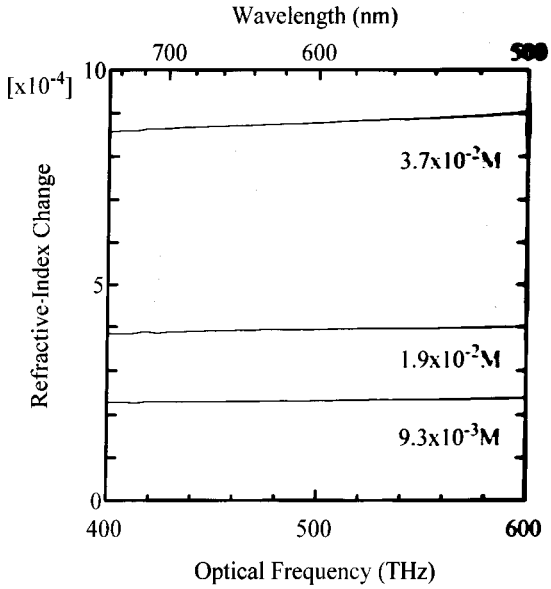

Fig. 3. Refractive-index spectrum of $CoCl_2$ in pyridine obtained from the measured interferograms. The concentrations of $CoCl_2$ are indicated.

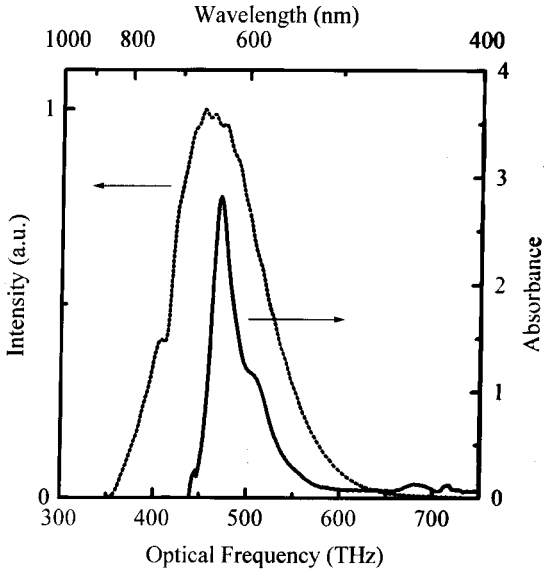

Fig. 4. Absorption spectrum of oxazine 1 in methanol (solid curve) and spectrum of the incident light (dotted curve).

interferes with the incident light to reduce the amplitude of the transmitted light. If the incident light is cut suddenly, the induced electric dipole moment decays with its own decay time while emitting the free-induction decay signal. The phase difference of π between the incident light and the free-induction decay signal is clearly seen in Fig. 5. Figure 6 shows the absorption spectrum and the spectrum of refractive index obtained by Fourier transformation of the measured interferograms. The agreement between the absorption spectrum thus obtained and that obtained with a conventional grating spectrometer is fairly good.

The third sample solution was nigrosine in water. Figure 7 shows the absorption spectrum and the spectral region of the measurement. In this case we reduced the spectral region of the measurement by inserting a color

glass filter in front of the input side of the Michelson interferometer so that it was well within the absorption spectrum of the sample solution. The autocorrelation and cross-correlation interferograms are shown in Fig. 8, where each interferogram is normalized at the peak. We see that the peak velocity of the light pulse increases with an increase of the solute concentration, unlike the case of $CoCl_2$ in pyridine. This is because in the case of $CoCl_2$ in pyridine the spectrum of measurement or incident light was in the normal-dispersion region, but in the case of nigrosine in water it is in the anomalous-dispersion region.

Electromagnetic-pulse propagation in an anomalous-dispersion region has attracted much attention.[8–14] The peak velocity exceeding the light speed in vacuum, c, is not contradictory to the special theory of relativity. In the region of strong anomalous dispersion the simple form of group velocity, which is expressed as

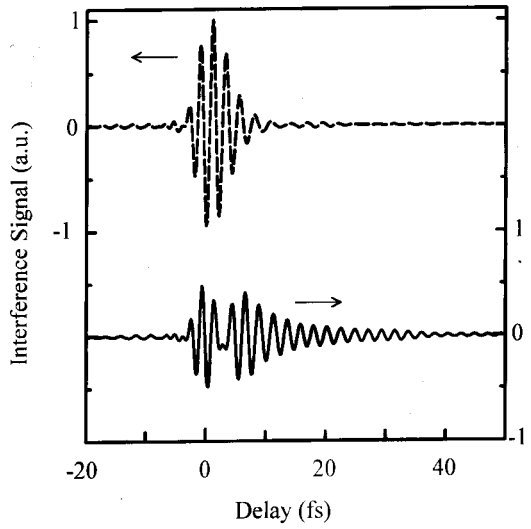

Fig. 5. Autocorrelation (dashed curve), and cross correlation (solid curve) of oxazine 1 in methanol (1.2×10^{-4} M).

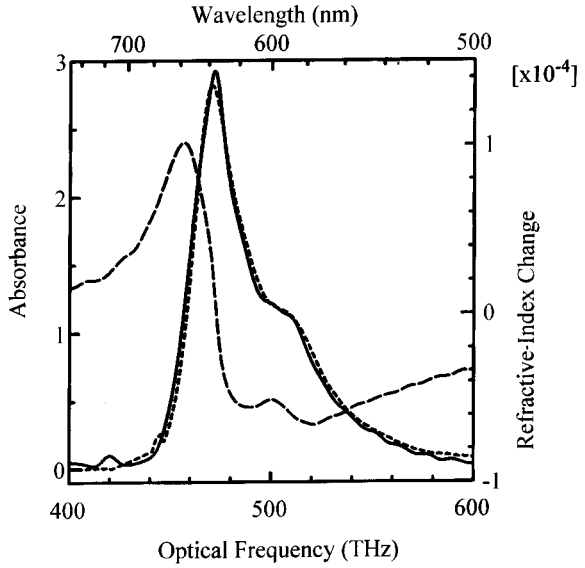

Fig. 6. Absorption spectrum (solid curve) and spectrum of refractive index (dashed curve) of oxazine 1 in methanol obtained from the measured interferograms. The absorption spectrum (dotted curve) obtained with conventional grating spectrometer is also shown.

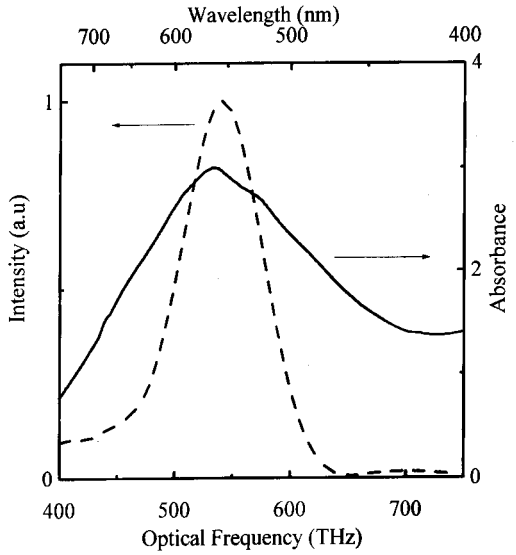

Fig. 7. Spectrum of incident light (dashed curve) and absorption spectrum (solid curve) of nigrosine in water (1.3×10^{-3} M).

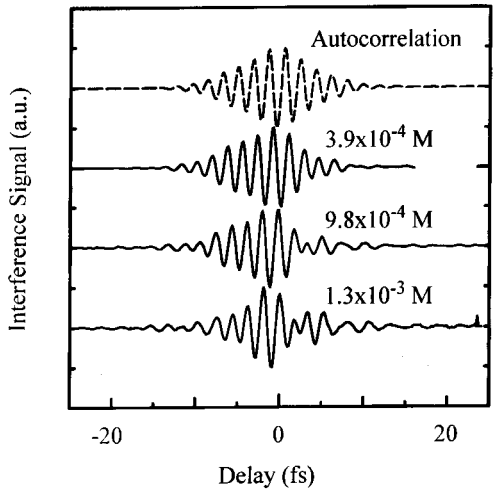

Fig. 8. Autocorrelation (dashed curve), and cross correlation (solid curves) of nigrosine in water. The concentrations of nigrosine are indicated.

$$v_g = \frac{d\omega}{dk} = \frac{c}{n(\omega) + \omega(dn(\omega)/d\omega)}, \tag{11}$$

can exceed c or even become negative. However, in this region the behavior of the pulse propagation becomes very complicated because of strong absorption. When the light pulse enters the sample, it is absorbed, and the electric dipole moment is induced. The electric field emitted by this electric dipole moment destructively interferes with the incident light to decrease the transmitted light intensity. However, it takes some time for the induced electric dipole moment to build up; hence the leading part of the light pulse accepts a relatively smaller absorption than does the other part of the light pulse. This is the reason for the increase of peak velocity in nigrosine in water or in the anomalous-dispersion region. If the solute concentration is further increased, the destructive interference between the incident light and the increased emitted light from the induced dipole moment results in the

formation of nodes in the trailing part of the transmitted waveform, as is shown in Fig. 8.

In the above discussion, we have simplified the deformation process of the waveform. It is not possible for each molecule to separate the light emitted by the sample from the incident light. For example, for the solute molecules located close to the output end of the glass cell, the already deformed waveform of light is the input waveform. Therefore, if the optical density of the sample is very large, the transmitted waveform becomes complicated even in the linear regime.

5. CONCLUSION

We have investigated linear propagation of light by using a white-light Michelson interferometer. The delay of pulse propagation was observed for a sample with normal dispersion. Free-induction decay signal was observed for a resonant sample that had a spectral width of absorption smaller than that of the incident light. Also, the increase of peak velocity was observed for a sample with anomalous dispersion. The complex transmission coefficients of the sample were also obtained by Fourier transformation of the obtained interferograms. The accuracy of our waveform measurement is demonstrated by the good agreement between the absorption spectrum obtained by Fourier transformation of the interferograms and that obtained by a conventional grating spectrometer.. If ultrashort laser pulses are used instead of incoherent light, Michelson interferometers can be applied to phase-sensitive ultrafast nonlinear spectroscopy.

REFERENCES

1. P. F. Barbara, W. H. Knox, B. A. Mourou, and A. H. Zewail, eds., *Ultrafast Phenomena IX* (Springer-Verlag, Berlin, 1994).
2. W. H. Knox, N. M. Pearson, K. D. Li, and C. A. Hirlimann, "Interferometric measurements of femtosecond group delay in optical components," Opt. Lett. **7**, 574–576 (1988).
3. K. Naganuma, K. Mogi, and H. Yamada, "Group-delay measurement using the Fourier transform of an interferometric cross correlation generated by white light," Opt. Lett. **15**, 393–395 (1990).
4. M. Beck and I. A. Walmsley, "Measurement of group delay with high temporal and spectral resolution," Opt. Lett. **15**, 492–494 (1990).
5. K. Naganuma and Y. Sakai, "Interferometric measurement of wavelength dispersion on femtosecond laser cavities," Opt. Lett. **19**, 487–489 (1994).
6. R. G. Brewer and R. L. Shoemaker, "Optical free induction decay," Phys. Rev. A **6**, 2001–2007 (1972).
7. N. Tsurumachi, T. Fuji, S. Kawato, T. Hattori, and H. Nakatsuka, "Interferometric observation of femtosecond free induction decay," Opt. Lett. **19**, 1867–1869 (1994).
8. L. Brillouin, *Wave Propagation and Group Velocity* (Academic, New York, 1960).
9. F. R. Faxvog, C. N. Y. Chow, T. Bieber, and J. A. Carruthers, "Measured pulse velocity greater than c in a neon absorption cell," Appl. Phys. Lett. **17**, 192–193 (1970).
10. C. G. B. Garrett and D. E. McCumber, "Propagation of a Gaussian light pulse through an anomalous dispersion medium," Phys. Rev. A **1**, 305–313 (1971).
11. M. D. Crisp, "Concept of group velocity in resonant pulse propagation," Phys. Rev. A **4**, 2104–2108 (1971).
12. S. Chu and S. Wong, "Linear pulse propagation in an absorbing medium," Phys. Rev. Lett. **48**, 738–741 (1982).
13. M. Tanaka, M. Fujiwara, and H. Ikegami, "Propagation of a Gaussian wave packet in an absorbing medium," Phys. Rev. A **34**, 4851–4858 (1986).
14. Y. Amagishi, H. Nakagawa, and M. Tanaka, "Ion-Neutral collision effect on an Alfvén Wave," Phys. Rev. Lett. **71**, 360–363 (1993).